Chapter 1

Introduction

1.1 Neutrino Oscillations

1.1.1 *Experiments*

The observation of neutrino oscillations has now established beyond doubt that neutrinos have mass and mix. This existence of neutrino masses is in fact the first solid experimental fact requiring physics beyond the Standard Model.

Since the early 1970s the chlorine solar neutrino experiment [1] provided evidence that electron neutrinos detected on earth were fewer than expected. In the 1980s this fact was confirmed by the water Čerenkov KamiokaNDE experiment [2] with a different detector threshold and the capability to demonstrate that the signals collected were indeed coming from the sun. A further experimental confirmation came in the early 1990s following two gallium experiments [3, 4] with very low detection thresholds. At the beginning of the 2000s, however, these experimental results were not considered evidence for neutrino oscillation, basically for two reasons: they were based on a comparison to theoretical predictions of the solar neutrino fluxes and multiple solutions could be found for the oscillation parameters, differing by several orders of magnitude to each other both in amplitude and in the neutrino mass difference squared.

This "solar neutrino puzzle" was closed in 2002 with the results from the SNO [5] and KamLAND [6] experiments. SNO, a heavy water Čerenkov solar neutrino detector, could simultaneously detect three solar neutrino processes: charged-current, elastic-scattering and neutral-currents, depending on different ratios of the ν_e and $\nu_\mu + \nu_\tau$ fluxes. In this way it was able to assess in a model-independent way that the total neutrino flux on earth (ν_e+ ν_μ+ ν_τ) was as expected while the ν_e flux (the only neutrino flavor generated on the sun) was indeed depleted, in a way compatible with the previous solar neutrino experiments. The KamLAND experiment provided at the same time a measurement of the disappearance of electron antineutrinos from nuclear fission reactors in Japan and Korea. This established, in combination with the solar neutrino results, large mixing-angle (LMA) MSW oscillations as the solution for the solar neutrino oscillations together with a precise determination of the relevant neutrino mixing angle and of the corresponding mass difference squared (see Table 1.1).

The first evidence of neutrino oscillation came from atmospheric neutrinos. Since the late 80s there have been indications from atmospheric neutrino experiments that muon neutrinos disappear when going through the earth. This was finally unambiguously demonstrated by the Super-Kamiokande experiment in 1998 [7], a result well supported by the Soudan2 [8] and MACRO [9] experiments. This disappearance takes place at a much shorter wavelength than for solar neutrinos (L/E$\sim$ 500 km/GeV) [10]; it is not seen for electron neutrinos, a fact that has been best established by the CHOOZ reactor experiment [11]. This disappearance has been confirmed by two long-baseline experiments: the K2K experiment in Japan [12] and MINOS in USA [13] (see Section 1.3.2).

A further, much more controversial, indication of $\overline{\nu}_\mu \to \overline{\nu}_e$ oscillations with a Δm^2 of 0.3 - 20 eV^2 came from the beam dump LSND experiment detecting a $\sim 4\sigma$ excess of $\overline{\nu}_e$ interactions in a neutrino beam produced by π^+ decays at rest where the $\overline{\nu}_e$ component was highly suppressed ($\sim 7.8 \cdot 10^{-4}$) [14]. The KARMEN experiment [15], using a very similar technique but with a lower sensitivity (a factor 10 less for the lower Δm^2), and the NOMAD experiment at WANF of CERN SPS [16], for $\Delta m^2 > 10$ eV^2, did not confirm the result, excluding a large part of the allowed region of the oscillation parameters. The results of the MiniBooNE experiment [17] again did not confirm the LSND result, even though some non-standard explanations, for instance sterile neutrinos [18] or ν_e disappearance [19], have not been fully excluded.

1.1.2 *Phenomenology*

The above experimental observations are consistently described by three families ν_1, ν_2, ν_3 with mass values m_1, m_2 and m_3 that are connected to the flavor eigenstates ν_e, $\nu_\mu$and ν_τ by a mixing matrix U, usually parameterized as

$$U(\theta_{12},\theta_{23},\theta_{13},\delta_{\rm CP}) = \begin{pmatrix} c_{13}c_{12} & c_{13}s_{12} & s_{13}e^{-i\delta_{\rm CP}} \\ -c_{23}s_{12} - s_{13}s_{23}c_{12}e^{i\delta_{\rm CP}} & c_{23}c_{12} - s_{13}s_{23}s_{12}e^{i\delta_{\rm CP}} & c_{13}s_{23} \\ s_{23}s_{12} - s_{13}c_{23}c_{12}e^{i\delta_{\rm CP}} & -s_{23}c_{12} - s_{13}c_{23}s_{12}e^{i\delta_{\rm CP}} & c_{13}c_{13} \end{pmatrix} \quad (1.1)$$

where the short-form notation $s_{ij} \equiv \sin\theta_{ij}, c_{ij} \equiv \cos\theta_{ij}$ is used. As a result, the neutrino oscillation probability depends on three mixing angles, $\theta_{12},\theta_{23},\theta_{13}$, two mass differences, $\Delta m^2_{12} = m^2_2 - m^2_1$, $\Delta m^2_{23} = m^2_3 - m^2_2$, and a CP phase $\delta_{\rm CP}$. Additional phases are present in case neutrinos are Majorana particles, but they do not influence neutrino flavor oscillations at all. Furthermore, the neutrino mass hierarchy, the order by which mass eigenstates are coupled to flavor eigenstates, can be fixed by measuring the sign of Δm^2_{23}. In vacuum the oscillation probability between two neutrino flavors α, β is:

$$P(\nu_\alpha \to \nu_\beta) = -4\sum_{k>j} Re[W^{jk}_{\alpha\beta}]\sin^2\frac{\Delta m^2_{jk}L}{4E_\nu} \pm 2\sum_{k>j} Im[W^{jk}_{\alpha\beta}]\sin^2\frac{\Delta m^2_{jk}L}{2E_\nu}, \quad (1.2)$$

where $\alpha = e,\mu,\tau,\ j = 1,2,3,\ W^{jk}_{\alpha\beta} = U_{\alpha j}U^*_{\beta j}U^*_{\alpha k}U_{\beta k}$. In the case of only two neutrino flavor oscillations it can be written as:

$$P(\nu_\alpha \to \nu_\beta) = \sin^2 2\theta\cdot \sin^2\frac{1.27\ \Delta m^2(eV^2)\cdot L(km)}{E_\nu(GeV)}. \quad (1.3)$$

When neutrinos pass through matter, the oscillation probability is perturbed [20] (see Eq. 1.5 in the following section). Two independent mass splittings characterize the system, since oscillations only depend on the difference of squared masses. Although no formally agreed definition exists, the usage is that the mass eigenstates are classified by decreasing electron-neutrino content $| < \nu_e|\nu_1 > |^2$, $| < \nu_\mu|\nu_2 > |^2$, $| < \nu_\tau|\nu_3 > |^2$. With this definition, the mass of ν_1 is not necessarily smaller than that of ν_2.

Since two-family neutrino oscillations in vacuum (Eq. 1.3) depend on the mass difference as $\sin^2(1.27\Delta m^2 L/E)$, one cannot determine the sign of Δm^2 unless the oscillation interferes with another process; in the case of electron neutrinos, this is offered by coherent scattering on electrons in matter, a.k.a. matter effects.

The best-fit values and allowed range of values of the oscillation parameters at different CL obtained in [22] are shown in Table 1.1.

Table 1.1 Best-fit values, 2σ, and 3σ intervals (1 dof) for the three flavor neutrino oscillation parameters from global data including solar, atmospheric, reactor (KamLAND and CHOOZ) and accelerator (K2K and MINOS) experiments [22].

parameter	best-fit	2σ	3σ
Δm^2_{21} $[10^{-5}\text{eV}^2]$	$7.65^{+0.23}_{-0.20}$	7.25–8.11	7.05–8.34
$\|\Delta m^2_{31}\|$ $[10^{-3}\text{eV}^2]$	$2.40^{+0.12}_{-0.11}$	2.18–2.64	2.07–2.75
$\sin^2\theta_{12}$	$0.304^{+0.022}_{-0.016}$	0.27–0.35	0.25–0.37
$\sin^2\theta_{23}$	$0.50^{+0.07}_{-0.06}$	0.39–0.63	0.36–0.67
$\sin^2\theta_{13}$	$0.01^{+0.016}_{-0.011}$	≤ 0.040	≤ 0.056

1.2 Three-family Oscillations and CP or T Violation

Three parameters have not yet been measured in neutrino oscillations: θ_{13} , sign(Δm^2_{23}) and δ_{CP}, all three fundamental parameters of the standard model.

The mixing angle θ_{13} is the key parameter of three-neutrino oscillations and regulates at the first order all the oscillation processes that could contribute to the measurement of sign(Δm^2_{23}) and δ_{CP}.

The sign(Δm^2_{23}) parameter is an internal degree of freedom in the neutrino sector; its value could be +1 (normal hierarchy), in which case ν_e would be the lightest neutrino, or -1 (inverted hierarchy), for which ν_e would be the heaviest (see Fig. 1.1). Its value is of great importance for double-beta decay experiments [23] and for great unification model building.

The CP phase δ_{CP} is the holy grail of ultimate neutrino oscillation searches. The demonstration of CP violation in the lepton sector (LCPV) and the knowledge of the value of this phase would be crucial to understanding the origin of the baryon asymmetry in the universe, providing a strong indication, though not proof, that leptogenesis is the explanation for the observed baryon asymmetry of the Universe [24].

All these parameters can be measured via subleading $\nu_\mu \to \nu_e$ oscillations that represent the key process of any future new discovery in neutrino oscillation physics.

The importance of precision measurements of the already measured neutrino parameters should not be underestimated. The atmospheric

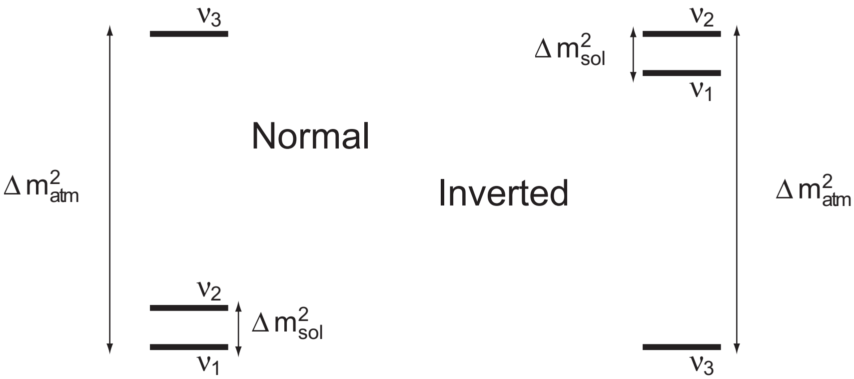

Fig. 1.1 The two three-neutrino mass schemes, normal and inverted hierarchy.

parameters can be precisely measured by long-baseline neutrino oscillation experiments via the $\nu_\mu \to \nu_\mu$ oscillation process.

1.2.1 *How to measure leptonic CP violation*

After the discovery of neutrino oscillations in 1998, it was soon realized that with three families and for a favorable set of parameters, it would be possible to observe violation of CP or T symmetries in neutrino oscillations [25]. This observation reinforced the considerable interest for precision measurements of neutrino oscillation parameters.

The year 2002 was very encouraging for LCPV projects, since the LMA solution emerged as the true solution for solar neutrino oscillations. Only for this solution can leptonic CP violation be large enough to be observed in high-energy neutrino oscillation appearance experiments.

This has led to extensive studies, such as those published in a CERN yellow report [26], the European Network BENE [27] or the International Scoping Study [28].

The phenomenon of CP (or T) violation in neutrino oscillations manifests itself by a difference in the oscillation probabilities of say, $P(\nu_\mu \to \nu_e)$ vs $P(\overline{\nu}_\mu \to \overline{\nu}_e)$ (CP violation), or $P(\nu_\mu \to \nu_e)$ vs $P(\nu_e \to \nu_\mu)$ (T violation).

It can be observed right away that observation of this important phenomenon requires appearance experiments; indeed a reactor or solar neutrino experiment, sensitive to the disappearance $P(\nu_e \to \nu_e)$ which is clearly time-reversal invariant, would be completely insensitive to it. This can be seen as an advantage in view of a precise and unambiguous measurement of the mixing angles; for the long-term goal of observing and studying CP violation, we are confined to appearance experiments.

The $\nu_\mu \to \nu_e$ transition probability in case of small matter effects can be parameterized as [29]:

$$\begin{aligned} P(\nu_\mu \to \nu_e) &= 4c_{13}^2 s_{13}^2 s_{23}^2 \sin^2 \frac{\Delta m_{13}^2 L}{4E_\nu} \times \left[1 \pm \frac{2a}{\Delta m_{13}^2}(1-2s_{13}^2)\right] \\ &+ 8c_{13}^2 s_{12} s_{13} s_{23} (c_{12}c_{23}\cos\delta_{\mathrm{CP}} - s_{12}s_{13}s_{23}) \cos\frac{\Delta m_{23}^2 L}{4E_\nu} \sin\frac{\Delta m_{13}^2 L}{4E_\nu} \sin\frac{\Delta m_{12}^2 L}{4E_\nu} \\ &\mp 8c_{13}^2 c_{12}c_{23}s_{12}s_{13}s_{23} \sin\delta_{\mathrm{CP}} \sin\frac{\Delta m_{23}^2 L}{4E_\nu} \sin\frac{\Delta m_{13}^2 L}{4E_\nu} \sin\frac{\Delta m_{12}^2 L}{4E_\nu} \\ &+ 4s_{12}^2 c_{13}^2 \{c_{13}^2 c_{23}^2 + s_{12}^2 s_{23}^2 s_{13}^2 - 2c_{12}c_{23}s_{12}s_{23}s_{13}\cos\delta_{\mathrm{CP}}\} \sin\frac{\Delta m_{12}^2 L}{4E_\nu} \\ &\mp 8c_{12}^2 s_{13}^2 s_{23}^2 \cos\frac{\Delta m_{23}^2 L}{4E_\nu} \sin\frac{\Delta m_{13}^2 L}{4E_\nu} \frac{aL}{4E_\nu}(1-2s_{13}^2). \end{aligned} \tag{1.4}$$

The first line of this parameterization contains the term driven by θ_{13}, the second and third contain CP even and odd terms respectively, and the fourth is driven by the solar parameters. The last line parameterizes matter effects developed at the first order where $a[\mathrm{eV}^2] = \pm 2\sqrt{2} G_F n_e E_\nu = 7.6{\cdot}10^{-5}\rho[g/cm^3]E_\nu[\mathrm{GeV}]$. The $\pm$ and $\mp$ terms refer to neutrinos and antineutrinos. A sketch of $P(\nu_\mu \to \nu_e)$ as a function of L for 1 GeV neutrinos is shown in Fig. 1.2.

When matter effects are not negligible, following Eq. (1) of [32], the transition probability $\nu_e \to \nu_\mu$ ($\bar\nu_e \to \bar\nu_\mu$) at second order in perturbation theory in θ_{13}, $\Delta m_{12}^2/\Delta m_{23}^2$, $|\Delta m_{12}^2/a|$ and $\Delta m_{12}^2 L/E_\nu$ (see also [20]) is:

$$P^{\pm}(\nu_e \to \nu_\mu) = X_\pm \sin^2(2\theta_{13}) + Y_\pm \cos(\theta_{13})\sin(2\theta_{13})\cos\left(\pm\delta - \frac{\Delta m_{23}^2 L}{4E_\nu}\right) + Z\,, \tag{1.5}$$

where $\pm$ refers to neutrinos and antineutrinos, respectively. The coefficients of the two equations are:

$$\begin{cases} X_\pm = \sin^2(\theta_{23})\left(\frac{\Delta m_{23}^2}{|a-\Delta m_{23}^2|}\right)^2 \sin^2\left(\frac{|a-\Delta m_{23}^2|L}{4E_\nu}\right)\,, \\ Y_\pm = \sin(2\theta_{12})\sin(2\theta_{23})\left(\frac{\Delta m_{12}^2}{a}\right)\left(\frac{\Delta m_{23}^2}{|a-\Delta m_{23}^2|}\right)\sin\left(\frac{aL}{4E_\nu}\right)\sin\left(\frac{|a-\Delta m_{23}^2|L}{4E_\nu}\right)\,, \\ Z = \cos^2(\theta_{23})\sin^2(2\theta_{12})\left(\frac{\Delta m_{12}^2}{a}\right)^2 \sin^2\left(\frac{aL}{4E_\nu}\right) \end{cases} \tag{1.6}$$

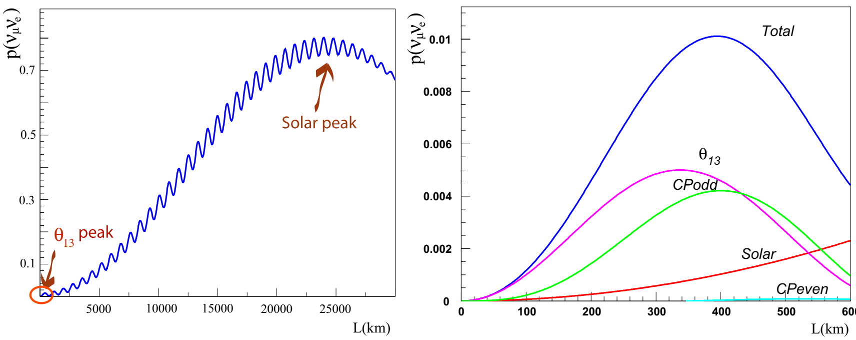

Fig. 1.2 Sketch of $P(\nu_\mu \rightarrow \nu_e)$ as function of the baseline computed for monochromatic neutrinos of 1 GeV in the solar baseline regime for $\delta_{\rm CP}$=0 (left) and in the atmospheric baseline regime for $\delta_{\rm CP} = -\pi/2$ (right), where the different terms of Eq. (1.4) are displayed. The following oscillation parameters were used in both cases: $\sin^2 2\theta_{13} = 0.01$, $\sin^2 2\theta_{12} = 0.8$, $\Delta m^2_{23} = 2.5{\cdot}10^{-3}$ eV^2, $\Delta m^2_{12} = 7{\cdot}10^{-5}$ eV^2. From Ref. [30].

Table 1.2 The 90%(3σ) bounds (1 dof) on $\sin^2\theta_{13}$ from an analysis of different sets of data read as [22]

$$\sin^2\theta_{13} \leq \begin{cases} 0.060\ (0.089) & \text{(solar+KamLAND)} \\ 0.027\ (0.058) & \text{(CHOOZ+atm+K2K+MINOS)} \\ 0.035\ (0.056) & \text{(global data)} \end{cases}$$

(remember that a changes sign by changing neutrinos with antineutrinos and that $P(\nu_e \rightarrow \mu_\mu, \delta_{\rm CP}) = P(\nu_\mu \rightarrow \nu_e, -\delta_{\rm CP})$).

θ_{13} searches look for experimental evidence of ν_e appearance in excess of what is expected from the solar terms. These measurements will be experimentally hard because the present limit on θ_{13} , summarized in Table 1.2, translates into a $\nu_\mu \rightarrow \nu_e$ appearance probability much smaller than 10% at the appearance maximum in a high energy muon neutrino beam.

One of the interesting aspects of Eq. (1.5) is the occurrence of matter effects which, unlike the straightforward θ_{13} term, depends on the sign of the mass difference sign(Δm^2_{23}). These terms should allow extraction of the mass hierarchy, but could also be seen as a background to the CP violating effect, from which they can be distinguished by the very different neutrino energy dependence, matter effects being larger for higher energies, with a "matter resonance" at about 12 GeV.

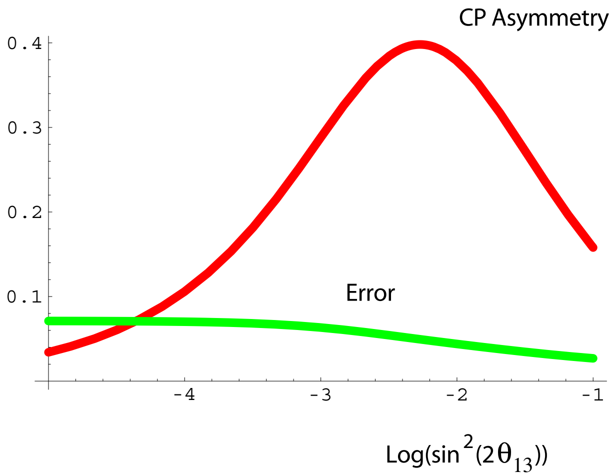

Fig. 1.3 Magnitude of the CP asymmetry at the first oscillation maximum, for $\delta = 1$ as a function of the mixing angle $\sin^2 2\theta_{13}$. The curve marked "error" indicates the dependence of the statistical+systematic error on such a measurement. The curves have been computed for the baseline beta beam option at the fixed energy $E_\nu = 0.4$ GeV, $L = 130$ km, statistical + 2% systematic errors. From [31].

The CP violation can be seen as interference between the solar and atmospheric oscillation for the same transition. Of experimental interest is the CP-violating asymmetry A_{CP}:

$$A_{CP} = \frac{P(\nu_\mu \to \nu_e) - P(\overline{\nu}_\mu \to \overline{\nu}_e)}{P(\nu_\mu \to \nu_e) + P(\overline{\nu}_\mu \to \overline{\nu}_e)} \tag{1.7}$$

displayed in Fig. 1.3, or the equivalent time reversal asymmetry A_T.

The asymmetry can be large and its value increases for decreasing values of θ_{13} until the two oscillations (solar and atmospheric) are of the same magnitude [31]. The following remarks can be made:

(1) Contrary to naive expectations, the most favorable θ_{13} values for LCPV searches are not the highest allowed.
(2) This asymmetry is valid for the first maximum. At the second oscillation maximum the curve is shifted to higher values of θ_{13} so that it can be then an interesting possibility for measuring the CP asymmetry, although the reduction in flux is considerable (roughly factor 9).
(3) The asymmetry has opposite signs for $\nu_e \to \nu_\mu$ and $\nu_e \to \nu_\tau$, which changes when going from one oscillation maximum to the next.
(4) The asymmetry is small for large values of θ_{13}, placing a challenging emphasis on systematics.

1.2.2 *The problem of degenerate solutions*

The richness of the $\nu_\mu \to \nu_e$ transition is also its weakness: it will be very difficult for pioneering experiments to extract all the genuine parameters unambiguously. Due to the three-flavor structure of the oscillation probabilities, for a given experiment several different disconnected regions of the multi-dimensional space of parameters could fit the experimental data, originating degenerate solutions.

Traditionally these degeneracies are referred to in the following ways:

- The *intrinsic* or $(\delta_{\rm CP}, \theta_{13})$-degeneracy [32]: for a measurement based on the $\nu_\mu \to \nu_e$ oscillation probability for neutrinos and antineutrinos, two disconnected solutions appear in the $(\delta_{\rm CP}, \theta_{13})$ plane.
- The *hierarchy* or sign(Δm^2_{31})-degeneracy [33]: the two solutions corresponding to the two signs of Δm^2_{31} appear in general at different values of $\delta_{\rm CP}$ and θ_{13}.
- The *octant* or θ_{23}-degeneracy [34]: since LBL experiments are sensitive mainly to $\sin^2 2\theta_{23}$ it is difficult to distinguish between the two octants $\theta_{23} < \pi/4$ and $\theta_{23} > \pi/4$. Again, the solutions corresponding to θ_{23} and $\pi/2 - \theta_{23}$ appear in general at different values of $\delta_{\rm CP}$ and θ_{13}.

This leads to an eight-fold ambiguity in θ_{13} and $\delta_{\rm CP}$ [35], and hence degeneracies provide a serious limitation for the determination of θ_{13}, $\delta_{\rm CP}$, and the sign of Δm^2_{31}. Discussions of degeneracies can be found for example in Refs. [36–39]; degeneracies in the context of the CERN–Fréjus beta beam and SPL have been considered for the first time in Ref. [40]. Degeneracies in the beta beam context are discussed in Section 3.5.2.

1.3 Experimental Setups

1.3.1 *Conventional neutrino beams*

Conventional neutrino beams are produced through the decay of π and K mesons generated by a high energy proton beam hitting small Z, needle-shaped, segmented targets. Positive (negative) mesons are sign-selected and focused (defocused) by large acceptance magnetic lenses into a long evacuated decay tunnel where ν_μ's ($\overline{\nu}_\mu$'s) are generated.

The length of the decay tunnel has to be optimized in order to maximize pion decays while keeping low the rate of muon decays, which contribute to the intrinsic ν_e beam contamination. Downstream the decay tunnel a beam

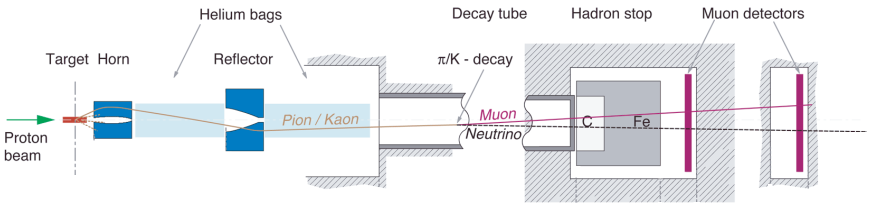

Fig. 1.4 Sketch of the CNGS neutrino beam line.

dump stops all the charged mesons while high energy muons are stopped downstream the beam dump by the earth: only neutrinos are allowed to reach the detector.

A not negligible fraction of the neutrinos hitting the detector is produced by secondary interactions in the target or in the material downstream. In case of positive charge selection, the ν_μ beam has typically a few percent of $\overline{\nu}_\mu$ contamination (from the decay of the residual π^-, K^- and K^0) and $\sim 1\%$ of ν_e and $\overline{\nu}_e$ coming from three-body $K^\pm$, K_0 decays and μ decays.

The precision of the evaluation of the intrinsic ν_e to ν_μ contamination is limited by the knowledge of the π and K production in the primary proton beam target. Hadroproduction measurements at 400 and 450 GeV/c performed with the NA20 [41] and SPY [42] experiments at the CERN SPS provided results with $5 \div 7\%$ intrinsic systematic uncertainties. The Harp experiment [43] measured both the K2K [44] and the MiniBooNE [45] targets, covering most of the useful pion phase-space, successfully improving the description of the two beam lines.

Close detectors are used to directly measure beam neutrinos and backgrounds this issue will be further discussed in Section 1.4.

1.3.2 *First generation long-baseline experiments*

The first generation of long-baseline (LBL) experiments focused on confirming the atmospheric evidence of oscillations and measuring $\sin^2 2\theta_{23}$ and $|\Delta m^2_{23}|$ within $10 \div 15\%$ of accuracy if $|\Delta m^2_{23}| > 10^{-3}$ eV^2. It was pioneered by the K2K experiment at KEK [12], which ended data taking in 2004 and confirmed the SuperKamiokande atmospheric oscillation evidence at 4.3σ.

K2K had a baseline of 250 km, and the muon-neutrino average energy was 1.2 GeV. The beam was created from a 12 GeV proton beam, 0.015 MW beam power. A dedicated close detector complex, with a 1 kt water Čerenkov tank, fine-grained detectors, and a muon ranger, was located 100 m from the end of the pion-decay volume. Super-Kamiokande was used as the far detector, and the first beam-induced neutrino event was observed in the summer of 1999. The final oscillation analysis [46] was performed using a data set corresponding to 0.922×10^{20} protons on target. Were observed 112 beam-originated neutrino events, where the expected number in the absence of oscillations was $158.1^{+9.2}_{-8.6}$. Of these events, 58 were single-ring muon-like events fully contained within the Super-Kamiokande detector. The energies and directions of the muons in fully contained events can be reconstructed, and because of the simple kinematics of the charged-current quasi-elastic (CCQE) events that make up much of the cross section around 1 GeV, it is possible to estimate the energy of the incoming neutrinos. Spectral distortions were in good agreement with the expectations derived from the neutrino disappearance. These results support maximal mixing, with best-fit two-neutrino oscillation parameters of $\sin^2 2\theta = 1$ and $\Delta m^2 = 2.8 \times 10^{-3}\text{eV}^2$. The 90% CL range for Δm^2 at $\sin^2 2\theta = 1$ is between 1.9 and 3.5 $\times10^{-3}\text{eV}^2$.

The MINOS (Main Injector Neutrino Oscillation Search) experiment was also proposed in 1995, with a neutrino beam, NuMI[47], pointed from Fermilab to the Soudan mine in Minnesota, with a baseline of 735 km. The beam has a system of movable focusing horns to allow the beam energy spectrum to be altered. Both near and far detectors consist of a steel and plastic scintillator sandwich structure.

The experiment started running in the spring of 2005, and within a year had gathered data corresponding to 2.50×10^{20} protons on target. The MINOS results support maximal mixing, with best-fit parameters of $|\Delta m^2| = (2.43 \pm 0.13) \times 10^{-3}\,\text{eV}^2$ and $\sin^2(2\theta) > 0.95$ at 68% confidence level [48].

The oscillation parameters from the K2K and MINOS experiments, together with results from SuperKamiokande are shown in Fig. 1.5. MINOS will run for five years, with the goal of accumulating 16×10^{20} protons on target. This data set should improve our knowledge of the oscillation parameters substantially. Both the experiments described here are linked, if only indirectly, to future projects to make precision measurements of the oscillation parameters and to probe the third mixing angle.

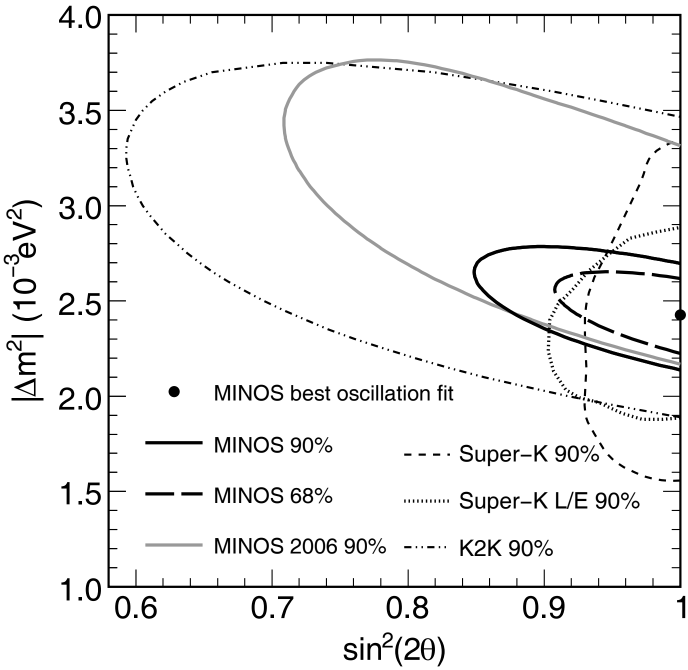

Fig. 1.5 Confidence intervals of atmospheric parameters as measured by MINOS, K2K and SuperKamiokande. From [48].

ICARUS [49] and OPERA [50] at the CNGS beam [51] from CERN to Gran Sasso laboratories will search for evidence of ν_τ interactions in a ν_μ beam, the final proof of $\nu_\mu \to \nu_\tau$ oscillations. CNGS had a first run in the 2006, while the OPERA detector started data taking with the full detector in 2008.

The CNGS ν_μ beam has been optimized for the $\nu_\mu \to \nu_\tau$ appearance search in order to overcome the kinematic threshold for τ production and to detect the τ decay products. The average neutrino energy, 17 GeV, is about ten times higher than the optimal value for θ_{13} searches at the CERN-LNGS baseline of 732 km.

Current long-baseline experiments with conventional neutrino beams can look for $\nu_\mu \to \nu_e$ oscillations (see Section 2) even if they are not optimized for such studies. MINOS at NuMI is expected to reach a sensitivity of $\sin^2 2\theta_{13} = 0.08$ [13] integrating $14{\cdot}10^{20}$ protons on target (pot) in five years according to the FNAL proton plan evolution [52]. MINOS's main limitation is the poor electron identification efficiency of the detector.

Thanks to the dense ECC structure and the high granularity provided by the nuclear emulsions, the OPERA detector is also suited for electron detection [50]. OPERA can reach a 90% CL sensitivity of $\sin^2 2\theta_{13} = 0.06$ ($\Delta m^2_{23} = 2.5{\cdot}10^{-3}$ eV^2, convoluted to CP and matter effects) [53], a factor ~ 2 better than CHOOZ for five years exposure to the CNGS beam at nominal intensity of $4.5{\cdot}10^{19}$ pot/yr.

1.3.3 *Second generation long-baseline experiments*

The focus of second generation LBL experiments will be the measurement of θ_{13} through the detection of sub-leading $\nu_\mu \to \nu_e$ oscillations.

According to the present experimental situation, conventional neutrino beams can be improved and optimized for the $\nu_\mu \to \nu_e$ searches. The design of a such new facility will demand higher neutrino fluxes, a neutrino beam optimized to the atmospheric Δm^2_{23} and a detector optimized to efficiently detect electrons and reject π°'s.

An interesting option for neutrino beams is the possibility to tilt the beam axis a few degrees with respect to the position of the far detector (off-axis beams) [54, 55]. According to the two-body π-decay kinematics, all the pions above a given momentum produce neutrinos of similar energy at a given angle $\theta \neq 0$ with respect to the direction of the parent pion (contrary to the $\theta = 0$ case where the neutrino energy is proportional to the pion momentum).

These neutrino beams have several advantages with respect to the corresponding on-axis ones: they are narrower, lower-energy and with a smaller ν_e contamination (since ν_e mainly come from three-body decays) although the neutrino flux can be significantly smaller.

In the next section the major players of this activity will be described, a sketch of θ_{13} sensitivities as a function of the time, following the schedule reported in the experimental proposals, is reported in Fig. 1.6.

1.3.3.1 *T2K*

The T2K (Tokai to Kamioka) experiment [54] will aim neutrinos from the Tokai site of J-PARC (50 GeV, 0.75 MW) to the Super-Kamiokande detector 295 km away. The neutrino beam is situated at an off-axis angle of 2.5 degrees, ensuring a pion decay peak energy of about 0.6 GeV. The beam line is equipped with a set of dedicated on-axis and off-axis near detectors

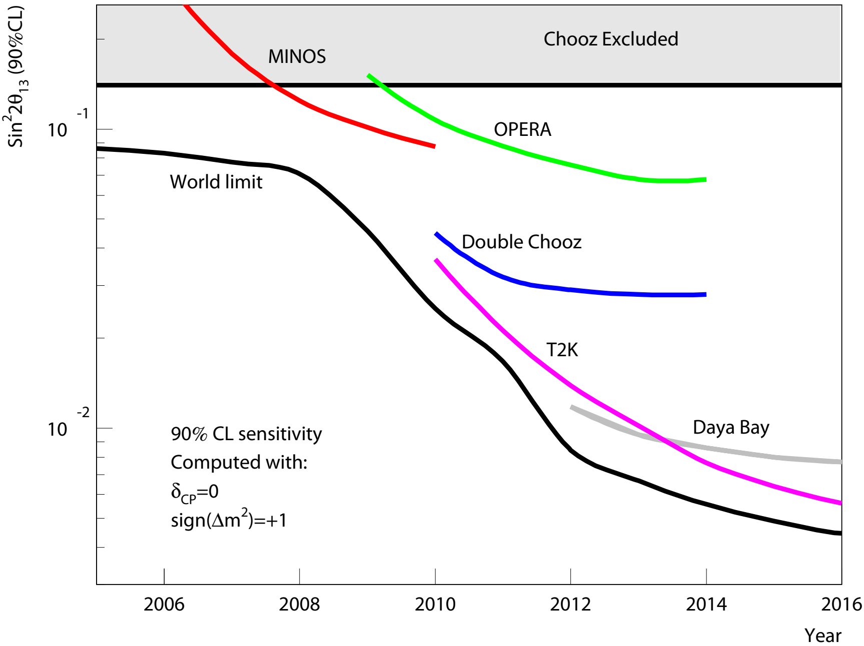

Fig. 1.6 Evolution of experimental $\sin^2 2\theta_{13}$ sensitivities as function of time. T2K sensitivity curve has been computed with the beam intensity curve of [56], Nova sensitivity is computed for 25 kt fiducial volume, $6.5 \cdot 10^{20}$ pot/yr, starting in 2012. Experiments are assumed to provide results after the first year of data taking.

at a distance of 280 m. In particular the off-axis near detector (ND280) will consist of finely segmented detectors acting as neutrino targets and tracking detectors surrounded by a magnet (recuperated from the UA1-NOMAD magnet at CERN). The purpose of the detector is to measure the neutrino spectrum, flux, ν_e contamination and interaction cross sections before the oscillation.

It is expected that the sensitivity of the experiment in a five-year ν_μ run, designed to begin on April 1, 2009, will be of the order of $\sin^2 2\theta_{13} \leq 0.006$ (90% CL).

T2K can also perform disappearance measurements of ν_μ, which will improve measurements of Δm^2_{23} to a precision of 0.0001 eV^2 or so. Neutral current disappearance (in events tagged by π° production) will allow for a sensitive search of sterile neutrino production.

1.3.3.2 *NOνA*

The NOνA experiment with an upgraded NuMI off-axis neutrino beam [57] ($E_\nu \sim 2$ GeV and a ν_e contamination lower than 0.5%) and with a baseline of 810 km (12 km off-axis), has been proposed at FNAL with the aim to explore $\nu_\mu \to \nu_e$ oscillations with a sensitivity 10 times better than MINOS. The experimental schedule at the moment is not well defined. The NuMI target will receive a 120 GeV/c proton flux with an expected intensity of $6.5{\cdot}10^{20}$ pot/year ($2{\cdot}10^7$ s/year are considered available to NuMI operations while the other beams are normalized to 10^7 s/year). The experiment will use a near and a far detector, both using liquid scintillator (TASD detectors). In a five-year ν_μ run with a 25 kt active mass far detector, a $\sin^2 2\theta_{13}$ sensitivity slightly better than T2K, as well as a precise measurement of $|\Delta m^2_{23}|$ and $\sin^2 2\theta_{23}$, can be achieved. NOνA can also allow the mass hierarchy problem to be solved for a limited range of the $\delta_{\rm CP}$ and sign(Δm^2_{23}) parameters [57], this thanks to the longer baseline with respect to T2K.

As a second phase, proton intensity could be raised up to $10 \cdot 10^{20}$ pot/yr and a second detector placed into operation at a different off-axis angle at the second oscillation maximum [57].

1.3.3.3 *Reactor experiments*

Another approach to searching for non-vanishing θ_{13} is to look at $\overline{\nu}_e$ disappearance using nuclear reactors as neutrino sources.

Reactor experiments aim at improving the current knowledge on θ_{13} by observing the disappearance of $\bar{\nu}_e$ from nuclear reactors. The relevant oscillation probability is

$$P(\bar{\nu}_e \to \bar{\nu}_e) \simeq 1 - \sin^2 2\theta_{13} \sin^2 \left(\frac{\Delta m^2_{31} L}{4E} \right) + \dots \qquad (1.8)$$

which does not depend on θ_{23} and the CP-phase δ_{CP}. The dependence on Δm^2_{21} and θ_{12} is negligible for the chosen baseline. Therefore this approach allows an unambiguous detection of θ_{13} free from correlations and degeneracies. As it is obvious from Eq. (1.8) the measurement requires a very precise control of the absolute flux. For that reason these experiments will employ a near and far detector. The direct comparison of the event rates in each detector will cancel many systematical errors and thus is essential in reaching the required low level of residual errors. Both detectors need some overburden to reduce the cosmic muon flux to an acceptable level.

The Double Chooz experiment, the follow-up to CHOOZ, will employ a far detector in the same location as the former CHOOZ detector as well as a near detector. Both detectors need some overburden to reduce the cosmic muon flux to an acceptable level. The advantage of Double Chooz is that it will use an existing cavern for the far detector, which puts it ahead of any other reactor experiment.

The sensitivity after five years of data taking will be $\sin^2 2\theta_{13} = 0.025$ at 90% CL [58], which could be achieved as early as 2012. It is conceivable to use a larger, second cavern to place a 200 t detector to further improve that bound down to $\sin^2 2\theta_{13} < 0.01$ [59].

The Daya Bay project in China [60] could reach a $\sin^2 2\theta_{13}$ sensitivity below 0.01 integrating 70 times the statistics of Double Chooz. This experiment will detect $\overline{\nu}_e$ produced by two pairs of reactor cores (Daya Bay and Ling Ao), separated by about 1.1 km. The complex generates 11.6 GW of thermal power; this will increase to 17.4 GW by early 2011 when a third pair of reactor cores (Ling Ao II) is put into operation.

It will consist of two near detector locations (each one with two 20 t detectors) and a far location consisting of four detectors of 20 t.

1.3.4 *Next generation conventional neutrino beams*

It is well-known today that T2K and NOνA, even if combined with a reactor experiment, will not be able to provide firm results (3σ or better) about leptonic CP violation [61] or sign(Δm^2_{23}) [62] whatever the value of θ_{13}. A next generation of long-baseline neutrino experiments will be needed to address this very important search in physics. The rule of thumb in such experiments is that they should be at least one order of magnitude more sensitive than T2K or NOνA. As a result they need an increase of two orders of magnitude on neutrino statistics with a consequent important reduction of systematic errors.

1.3.4.1 *Neutrino super beams*

To fulfill such a challenging improvement, conventional neutrino beams must be pushed to their ultimate limits (neutrino super beams) [29] and gigantic (megaton scale) neutrino detectors must be built.

In the following, a super beam is taken to be a conventional neutrino beam driven by a proton driver with a beam power in the range of 2-5 MW.

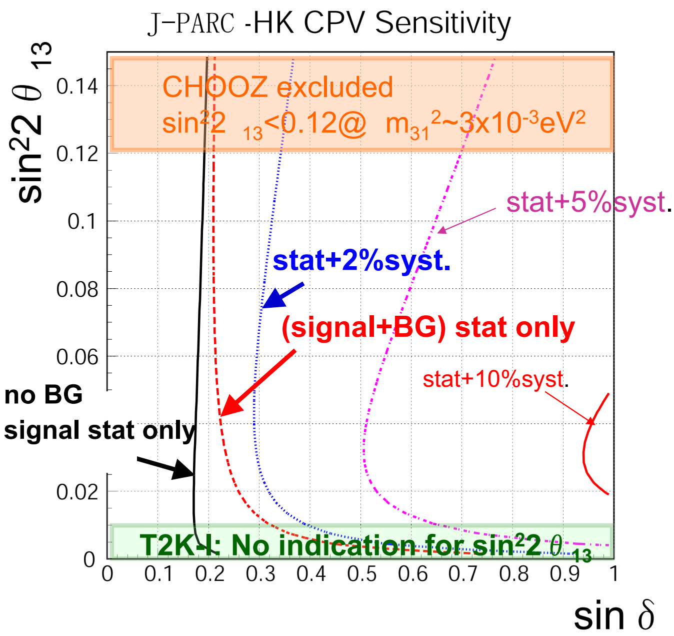

Fig. 1.7 LCPV sensitivity curve of T2HK. From [63].

1.3.4.2 *T2HK and T2KK*

Phase II of the T2K experiment, often called T2HK, foresees an increase of beam power up to the maximum feasible with the accelerator and target (4 MW beam power), antineutrino runs, and a very large, 520 kt, water Čerenkov, HyperKamiokande or HK, to be built close to SuperKamiokande.

Performances of such a setup have been computed in Ref. [63] (see Fig. 1.7). From this figure two main considerations can be taken:

(1) Systematic errors play a critical role in LCPV sensitivities: systematic errors bigger than 5% could potentially kill the experimental sensitivity. For a detailed discussion of systematic errors in T2HK and the possible role of ancillary experiments to reduce them, see [64].
(2) For θ_{13} values smaller than the T2K phase I sensitivity, T2HK has no sensitivity to LCPV. That is in case of a null result of T2K which would severely compromise the physics case of T2HK.

An evolution of T2HK is the T2KK project, where half of the HK detector would be installed in Japan, while the second half would be mounted in Korea, at a baseline of about 900 km, around the second oscillation maximum. This configuration would have worse sensitivities to θ_{13} with respect to T2HK, very similar sensitivities to LCPV and much better sensitivities to sign(Δm^2_{23}). For further details of this project see [65].

1.3.4.3 *CNGS upgrades*

Sensitivities for an upgraded CNGS setup have been first computed in [66]. The experimental setup can be summarized as follows:

- A proton intensity of $4.1 \cdot 10^{20}$ pot/yr has been assumed, to be compared with the nominal CNGS intensity of $4.5 \cdot 10^{19}$ pot/yr [1].
- To be at the first maximum at a baseline of around 750 km, the beam optics has been re-designed to focus pions of about 10 GeV/c momentum, against the 35 GeV/c momentum of the nominal CNGS. Several different off-axis angles have been taken into account.
- A monolythic 100 kt liquid argon detector (ICARUS actually is composed by two tanks of 300 kt) should be installed at shallow depth at a baseline of about 800 km.

With this setup, in a ten-year $\nu_\mu + \overline{\nu}_\mu$ run a sensitivity of $\sin^2 2\theta_{13} \geq 1 \cdot 10^{-3}$ ($3\ \sigma$, $\delta_{\rm CP}$=0, sign(Δm^2_{23})=+1) could be reached.

A subsequent LoI, MODULAr [68], has been proposed by the ICARUS collaboration for a similar setup: 1.2-$4.3 \cdot 10^{20}$ pot/yr and a modular 20 kt liquid argon detector to be installed at shallow depth at a baseline of 732 km, 10 km off-axis. This project could reach a sensitivity of $\sin^2 2\theta_{13} \geq 2.5 \cdot 10^{-3}\quad (3\sigma)$, $\delta_{\rm CP}$=0, in five years of neutrino operation.

1.3.4.4 *CERN-SPL*

In the CERN-SPL super beam project [69, 70] the planned 4MW SPL (Superconducting Proton Linac) would deliver a 3.5 GeV/c H^- beam on a Hg target to generate a neutrino beam with an average energy of ~ 0.3 GeV [2].

[1] According to the CERN report [67], the ultimate CNGS intensity, having changed the whole SPS injection chain, substituted the SPS RF cavities and upgraded the CNGS instrumentation, would be $1.3 \cdot 10^{19}$ pot/yr, or $2.45 \cdot 10^{19}$ pot/yr if all the fixed target programmes at CERN were canceled.

[2] At present SPL is foreseen as one of the elements of a new injection chain for the SPS, in view of the LHC luminosity upgrades [71]. In this context a power of 0.4 MW would be enough. Extensions to 4 MW could be driven by the needs of a neutrino super beam

The ν_e contamination from K will be suppressed by threshold effects and the resulting ν_e/ν_μ ratio ($\sim 0.4\%$) will be known within 2% error. The use of a near and far detector (the latter at $L = 130$ km in the Fréjus area, see Section 1.3.4.6) will allow for both ν_μ-disappearance and $\nu_\mu \to \nu_e$ appearance studies. The physics potential of the SPL super beam (SPL-SB) with a water Čerenkov far detector with a fiducial mass of 440 kt, has been extensively studied [72–75].

The most updated sensitivity estimations for this setup have been published in Ref. [76] and are shown in Section 3.7.

1.3.4.5 *Wide-band super beam*

A wide-band beam (WBB) has been proposed, sited at BNL and serving a very long-baseline experiment [77]. In this proposal, the 28 GeV AGS would be upgraded to 1 MW and a neutrino beam with neutrino energies in the range 0 - 6 GeV could be sent to a Megaton water Čerenkov detector at the Homestake mine at a baseline of 2540 km.

Wide-band beams possess the advantages of a higher on-axis flux and a broad energy spectrum. The latter allows the first and second oscillation nodes in the disappearance channel to be observed, providing a strong tool to solve the degeneracy problem. On the other hand, experiments served by wide-band beams must determine the incident neutrino energy with good resolution and eliminate the background from the high energy tail of the spectrum.

Upgrades to the FNAL main injector after the end of the Tevatron programme are also under study and could provide a similar wide-band neutrino beam. The baseline in this case would be 1290 km.

The combination of channels and spectral information of a long-baseline wide-band beam experiment offers a promising means of solving parameter degeneracies. However, the very long-baseline decreases the event rate at the far detector and reduces the sensitivity of the experiment to θ_{13} and CP-violation; the sensitivity of the experiment to θ_{13} and δ is somewhat smaller than that of T2HK or the SPL.

The wide-band beam is a very interesting option to search for the sign(Δm^2_{23})value and for leptonic CP-violation, solving most of the degeneracies, if θ_{13} is large enough, i.e. $\sin^2 2\theta_{13} > 5 \times 10^{-3}$ ($\theta_{13} > 2°$).

---

or a proton driver for a neutrino factory and/or a proton driver for EURISOL.

1.3.4.6 *Water Čerenkov detectors and the MEMPHYS detector*

For small values of θ_{13}, a very large data set is required for the sub-leading $\nu_\mu \to \nu_e$ oscillation to be observed. The water Čerenkov is an ideal detector for this task since it is possible to construct a detector of very large fiducial mass in which the target material is also the active medium. The Čerenkov light is collected by photo-detectors distributed over the surface of the detector; the cost of instrumenting the detector, therefore, scales with the surface area rather than the fiducial mass. Megaton-class water Čerenkov detectors are therefore ideal when charge identification is not required and have been chosen for T2HK, the SPL super beam, and the long-baseline wide-band beam experiment. Such a device could also be the ultimate tool for proton-decay searches and for the detection of atmospheric, solar, and supernovæneutrinos.

Charged leptons are identified through the detection of Čerenkov light in photo-multiplier tubes (PMTs) distributed around the vessel. The features of the Čerenkov rings can be exploited for particle identification. A muon scatters very little in crossing the detector, therefore, the associated Čerenkov ring has sharp edges. Conversely, an electron showers in the water, producing rings with "fuzzy" edges. The total measured light can be used to give an estimate of the lepton energy, while the time measurement provided by each PMT allows the lepton direction and the position of the neutrino interaction vertex to be determined. By combining all this information, it is possible to reconstruct the energy, the direction, and the flavor of the incoming neutrino. It is worth noting that the procedure discussed above is suitable only for quasi-elastic events ($\nu_l n \to l^- p$). Indeed, for non-quasi-elastic events more particles present in the final state are either below the Čerenkov threshold or are neutral, resulting in a poor measurement of the total event energy. Furthermore, the presence of more than one particle above threshold produces more than one ring, spoiling the particle identification capability of the detector.

The MEMPHYS (Megaton Mass Physics) detector [78] is a megaton-class water Čerenkov in straight extrapolation of the well-known and robust technique used for the Super-Kamiokande detector. It is designed to be located at Fréjus, 130 km from CERN, and is an alternative design of the UNO [79] and Hyper-Kamiokande [54] detectors and shares the same physics case in both the non-accelerator domain (nucleon decay, SuperNovae neutrino from burst event or from relic explosion, solar and atmospheric neutrinos) and the accelerator (super beam, beta beam) domain [185].

MEMPHYS may be built with current techniques near the present Modane Underground Laboratory as three- or four-shaft modular detector, with shafts of 250000 m^3 each, measuring 65 m in diameter, 65 m in height for the total water containment. Each of these shafts corresponds to about five times the present Super-Kamiokande cavity. For the current physical study, a fiducial volume of 440 kt which means three shafts and an Inner Detector (ID) 57 m in diameter and 57 m in height is assumed. A sketch of the possible layout of the laboratory is displayed in Fig. 1.8. Each ID may be equipped with photodetectors (PMT, HPD,..) with a surface coverage of at least 30%. The Fréjus site, 4800 m.w.e, offers a natural protection against cosmic rays by a factor of about 10^6.

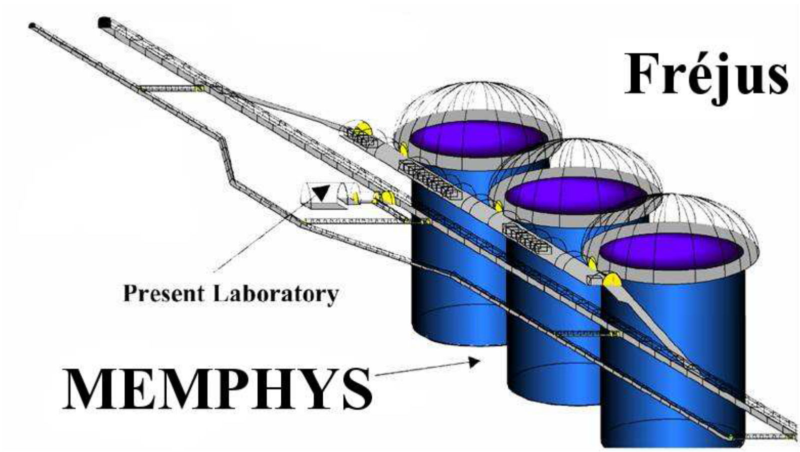

Fig. 1.8 Possible layout of the future Fréjus underground laboratory.

1.4 Why Look For New Concepts in Neutrino Beams?

The event collected in a neutrino oscillation detector, N^{far}_{events}, can be described by the following equation:

$$N^{far}_{events} = \left(\sigma_{\nu_e}\epsilon_{\nu_e}P_{\nu_\mu\nu_e} + \sigma^{NC}_{\nu_\mu}\eta_{NC} + \sigma^{CC}_{\nu_\mu}\eta_{CC}P_{\nu_\mu\nu_\mu}\right)\Phi_{\nu_\mu} + \sigma^{CC}_{\nu_e}\epsilon_{\nu_e}\Phi_{\nu_e} \quad (1.9)$$

where

- $\sigma_\nu(E_\nu)$ is the cross section of ν
- $\epsilon_{\nu_e}(E_\nu)$ is the detection efficiency of electron neutrinos
- $P_{\nu_\mu\nu_e}(E_\nu)$, $P_{\nu_\mu\nu_\mu}(E_\nu)$ are oscillation probabilities
- $\eta_{NC(CC)}(E_\nu)$ is the detection efficiency of backgrounds from NC (CC) $\nu_\mu$interactions.
- $\Phi_{\nu_\mu}(E_\nu)$ is the $\nu_\mu$flux at the detector
- $\Phi_{\nu_e}(E_\nu)$ is the ν_e flux at the detector
- Cross section and fluxes are not known to better than 5%.

A close detector placed near enough the neutrino target to consider the oscillation probabilities negligible would measure

$$\mathrm{N}^{\mathrm{close}}_{\mathrm{events}} = \left(\sigma^{\mathrm{NC}}_{\nu_\mu}\eta'_{\mathrm{NC}} + \sigma^{\mathrm{CC}}_{\nu_\mu}\eta'_{\mathrm{CC}}\right)\Phi'_{\nu_\mu} + \sigma^{\mathrm{CC}}_{\nu_\mathrm{e}}\epsilon_{\nu_\mathrm{e}}\Phi'_{\nu_\mathrm{e}} \tag{1.10}$$

where the background efficiencies $\eta'_{NC(CC)}(E_\nu)$ are not necessarily the same as the far detector, and more important the neutrino fluxes $\Phi'_{\nu_\mu}(E_\nu)$ and $\Phi'_{\nu_e}(E_\nu)$ are not the same as the far detector. This latter phenomenon is due to the fact that the close detector is sensitive to the length of the decay tunnel, and for simple solid angle considerations is more sensitive to pions that decay late in the tunnel, the most energetic, while the far detector is insensitive to this geometrical factor. This effect produces differences between the close and far detector neutrino fluxes of up to 30%.

It is clear that a close detector cannot constrain all the single variables that contribute to the far detector signal rate, but first generation neutrino beams have demonstrated that it is still quite powerful in controlling systematic errors, especially if coupled with measurements of the pion production rates at the target (hadroproduction experiments) that can efficiently constrain the prediction of the neutrino flux both at the close and at the far detector sites. A quantitative discussion about the effects of the close detectors on neutrino super beam experiments can be found in [64].

With the close detector data the K2K experiment concluded the $\nu_\mu \to \nu_e$ search with an overall 30% systematic error [80]. This value could be improved by using the Harp hadroproduction data [44], as already done for the ν_μ disappearance measurements of K2K.

The NOMAD experiment at CERN [81] was indeed able to predict the ν_e spectrum with a 5% systematic error [82]; this prediction was then successfully cross-checked with data [16]. The NOMAD experiment did not have a close detector but had the unprecedented capability of measuring with large statistics and good precision all four neutrino flavors (ν_μ, $\overline{\nu}_\mu$, ν_e, $\overline{\nu}_e$) in a ν_μ beam, a $\overline{\nu}_\mu$ beam and a neutrino beam without any horn focusing. The ν_μ, $\overline{\nu}_\mu$, $\overline{\nu}_e$ measurements in such conditions were basically enough to constrain the MC predictions of most secondary mesons in the neutrino beam line (π^-, π^+, k^-, k^+, k°), reducing most of the systematic errors in the ν_e prediction.

The T2K experiment expects to push the systematics below 10%, thanks to an improved close detector system 280 m downstream the target. It will use detectors in a magnetic field to isolate the single neutrino flavors, and specialized detectors for the different backgrounds, in particular a specialized detector for the NC π° background. A second close detector station is under evaluation at a distance of 2 km from the target. At such a distance the neutrino fluxes are quite similar to the far detector fluxes and a water Čerenkov detector can be safely put into operation. This second station could be very powerful in further reducing the systematics.

The goal to constrain the systematics to less than 5% appears quite challenging in conventional neutrino beams. Many systematics that at first order cancel out in a close-far detector ratio contribute at the second order if the level of systematic errors is fixed at 5% or below, forcing the need to independently measure any single variable of Eq. (1.9).

Two main problems appear particularly critical from this perspective:

- The neutrino flux is necessary in any cross section and efficiency measurement. It requires a precise measurement of the neutrino hadroproduction at the target and a precise simulation of all the primary and secondary reinteractions in the target itself and in all the materials of the neutrino beam line. It should be noted that the best hadroproduction measurement published so far, the Harp measurement of the MiniBooNE beryllium target, concluded the analysis with a 4.9% integral systematic error and 9.8% differential systematic error [45].
- Conventional neutrino beams always produce at least four neutrino flavors (ν_μ, ν_e, $\overline{\nu}_\mu$, $\overline{\nu}_e$), of which ν_e and $\overline{\nu}_e$ are an intrinsic irreducible background for any $\nu_\mu \to \nu_e$ search, while $\overline{\nu}_\mu(\nu_\mu)$ are a background for any CP search.

1.5 New Concepts on Neutrino Beams

The intrinsic limitations of conventional neutrino beams can be overcome if the neutrino parents are fully selected, collimated and accelerated to a given energy.

With this challenging approach several important improvements can be made to conventional neutrino beams:

- The neutrino fluxes would be simply derived from the knowledge of the number of parents circulating in the decay ring and from their Lorentz boost factor γ.
- The intrinsic neutrino backgrounds would be suppressed (in the case of beta beam) or reduced to wrong sign muons (golden channel in neutrino factories).

The technological problems derive from the fact that the parents need to be unstable particles, requiring a fast, efficient acceleration scheme.

This can be attempted within the muon lifetime, bringing to the neutrino factories [83], or within beta decaying ion lifetimes, bringing to the beta beam [85].

With this kind of beams (in the specific case of a beta beam) the number of events in the far detector would be given by

$$\mathrm{N}_{\mathrm{events}}^{\mathrm{far}} = \left(\sigma_{\nu_\mu}\epsilon_{\nu_\mu}\mathrm{P}_{\nu_\mathrm{e}\nu_\mu} + \sigma_{\nu_\mathrm{e}}^{\mathrm{NC}}\eta_{\mathrm{NC}} + \sigma_{\nu_\mathrm{e}}^{\mathrm{CC}}\eta_{\mathrm{CC}}\mathrm{P}_{\nu_\mathrm{e}\nu_\mathrm{e}}\right)\phi_{\nu_\mathrm{e}}\,. \tag{1.11}$$

And in the close detector:

$$\mathrm{N}_{\mathrm{events}}^{\mathrm{close}} = \left(\sigma_{\nu_\mathrm{e}}^{\mathrm{NC}}\eta'_{\mathrm{NC}} + \sigma_{\nu_\mathrm{e}}^{\mathrm{CC}}\eta'_{\mathrm{CC}}\right)\phi_{\nu_\mathrm{e}}\,. \tag{1.12}$$

As a consequence:

- There is no need to disentangle NC from $\nu_\mu$events at the close detector, since $\nu_\mu$events are absent.
- Even if the close and far detector neutrino fluxes are different, they are fully predictable, so there is no need for a hadroproduction experiment with its associated errors.
- It should anyway be noted that the absence of ν_μ events in the close detector means that there is no way to measure signal (ν_μ) cross sections in the close detector. This could represent the major source of systematic errors in a beta-beam experiment.

1.5.1 *Neutrino factories*

In a neutrino factory the neutrinos originate from the decay of muons which are created via pions by protons impinging on a target. The muons have to be captured, cooled, accelerated and put into a decay ring with straight sections pointing towards the detectors.

The muon decay is well understood. Consequently, the composition and spectral characteristics of the resulting neutrino beam can be calculated with high precision. Furthermore, the use of a decay ring will result in a well collimated neutrino beam. The intensity will scale with the power of the driver beam but it will also depend heavily on the efficiency of the capture and cooling schemes and the swiftness of the acceleration as muons are very short lived.

The IDS study [84] aims at 5×10^{20} neutrinos along the straight sections of two independent storage rings of 25 GeV. This would require a driver beam intensity of some 4 MW at 5-10 GeV depending on the driver type. The target can either be a fast rotating solid target or a liquid metal target. Even metal power targets have been considered. Approximately a third of the driver beam power will be absorbed in the target with the remianing beam power being lost in a beam dump downstream of the target.

The pions emerging from the target are captured with a magnetic horn or a superconducting solenoid. The muons from the pion decay are cooled in an cooling channel in which ionization cooling is applied to reduce the beam emittance. The resulting muon beam is accelerated with recirculating linacs and a Fixed Field Alternating Gradient accelerator and finally stoored in two independent race track stoarge rings with straight sections of some 600 meter.